JACS
JOURNAL OF THE AMERICAN CHEMICAL SOCIETY
Article
pubs.acs.org/JACS

Highly Fluorescent Chameleon Nanoparticles and Polymer Films: Multicomponent Organic Systems that Combine FRET and Photochromic Switching

Sanghoon Kim, Seong-Jun Yoon, and Soo Young Park*

Center for Supramolecular Optoelectronic Materials and WCU Hybrid Materials Program, Department of Materials Science and Engineering, Seoul National University, Seoul 151-744, Korea

Supporting Information

ABSTRACT: We describe the preparation of highly efficient stimulus-responsive fluorescence color-tuning in self-assembled supramolecular scaffold systems. The systems consisted of a photochromic compound (BP-BTE) in combination with unique luminescent organic materials (CN-MBE, TPS-CNMBE, TPA-2CNMBE) that exhibited intense fluorescence in the solid state. The emission spectrum was tuned by introducing fluorescence resonance energy transfer and photochromic switching capabilities into the system. The materials were used to successfully demonstrate novel fluorescence patterns that were responsive to multiple stimuli, displayed reversible fluorescence switching, and provided a nondestructive readout of the fluorescence signal.

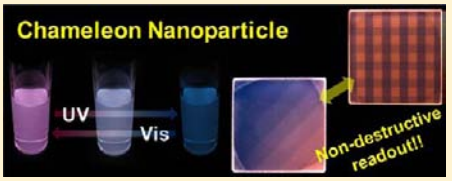

INTRODUCTION

Highly fluorescent π-conjugated organic compounds show promise in a wide range of applications, including electronic displays, lasing, sensing, biochemical imaging, and labeling. In principle, fluorescence emission spectra are determined by the frontier energy levels of the emitter. Thus, luminescence color tuning is generally achieved by varying the chemical structure of a molecular emitter, with particular emphasis on the π-conjugation length, annulation of the aromatic ring, and intramolecular charge-transfer interactions between the electron-donating and/or electron-accepting substituent.[1]

An alternative method for tuning fluorescence emission spectra involves constructing a two-component emitter system, in which fluorescence resonance energy transfer (FRET) is precisely modulated by the ratio of and distance between the donor and acceptor components. FRET methods provide a convenient means for color tuning over a spectral range bounded by the isolated donor and acceptor spectra.[2] A variety of systems utilizing FRET methods have been reported, including conjugated polymer nanoparticles,[3] silica nanoparticles,[4] and polymer micelle films.[5] These systems have found applications ranging from biological imaging and labeling to electronic display. Beyond passively tuning the fluorescence emission spectrum, the sensitivity of FRET signals to environmental conditions may be exploited in stimulus-responsive detection applications, including thermal-,[6] photo-,[7] vapor-,[8] and combinations of stimuli.[9] Such applications draw increasing attention for their utility in biosensors and optical memory devices.[10]

Among the various FRET-controlled fluorescence color tuning systems explored thus far, self-assembled nanostructure scaffolds that incorporate small molecule donor−acceptor fluorophores are expected to demonstrate the highest FRET efficiencies. Mixed fluorophores can be arrayed in a regular arrangement through self-assembly processes that provide ideal conditions of spatial proximity between donor and acceptor units within a nanostructure scaffold, thereby guaranteeing highly efficient energy transfer. To this end, a high fluorescence quantum yield in the solid state and a well-defined route to fluorophore self-assembly are critical for successful color tuning, as demonstrated in several molecular systems.[11] Stimulus-responsive FRET sensors that yield chameleon-like fluorescence color variations in a single nanostructured scaffold have not yet been explored, despite the tremendous application potential.[12]

Herein, we describe stimulus-responsive FRET modulation in highly emissive self-assembled nanostructures comprising a functional mixture of π-conjugated small molecules, including nanoparticles dispersed in an aqueous medium and in a polymer matrix (Figure 1). These systems consist of π-conjugated fluorescent donor, acceptor, and photochromic compounds that participate to different degrees in the self-assembly and FRET processes. The FRET efficiency was controlled by varying the distance between donors and acceptors either by varying the donor−acceptor ratio or by promoting donor-selective self-assembly via solvent−vapor annealing (SVA). Energy level switching was achieved by photoinduced interconversion of the photochromic compound, which acted as an alternative FRET acceptor. The overall goal is to achieve versatile and stimulus-responsive fluorescence color tuning in multicomponent nanoparticles via enhancing or suppressing FRET, which not only provides scientific meaning but also has practical application in optical recording and sensing.

Received: March 21, 2012
Published: June 29, 2012

   dx.doi.org/10.1021/ja3027295 | J. Am. Chem. Soc. 2012, 134, 12091−12097

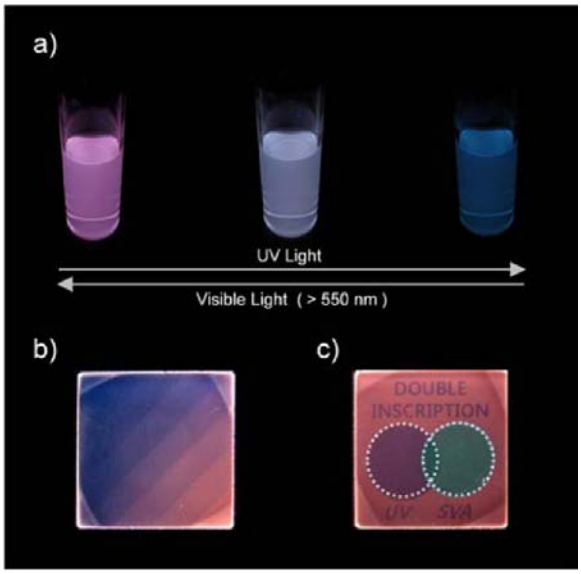

Figure 1. (a) Photoresponsive reversible fluorescence image of a CN-MBE/TPA-2CNMBE/BP-BTE nanoparticles suspension system. (b) Color gradient fluorescence image of a CN-MBE/TPA-2CNMBE/BP-BTE-doped polymer film system, patterned using photostimuli. (c) Fluorescence image of a CN-MBE/TPA-2CNMBE/BP-BTE-doped polymer film system that was doubly inscribed using photostimuli and vapor stimuli. The left and right white dashed circles indicate UV-light-exposed and solvent−vapor-exposed regions, respectively.

RESULTS AND DISCUSSION

Strong fluorescence emission in a self-assembled nanostructure is a required feature of fluorescent compounds suitable for the FRET system described here. Such compounds should yield a high quantum yield and efficient FRET with minimal concentration quenching in condensed phases. Accordingly, we synthesized three unique π-conjugated compounds that exhibited extraordinarily intense fluorescence in the solid state. These compounds displayed a dramatically enhanced fluorescence efficiencies via aggregation-induced enhanced emission (AIEE).[13] (*Z*)-2,3-bis(4′-methyl-[1,1′-biphenyl]-4-yl)-acrylonitrile (CN-MBE, Scheme 1a) was synthesized according to the method described in the literature and used as a FRET donor. CN-MBE exhibited bright greenish-blue emission in the solid state, together with exceptional self-assembly into fluorescent nanoparticles.[13a] (*Z*)-2,3-bis(4′-(triphenylsilyl)-[1,1′-biphenyl]-4-yl)acrylonitrile (TPS-CNMBE, Schemes 1b and S1 and Figure S1, Supporting Information (SI)) was newly designed and synthesized as an alternative FRET donor. CNMBE also exhibited greenish blue emission in the solid state, similar to CN-MBE, with a much weaker tendency to self-assemble, probably due to steric effects among the tetraphenylsilane groups. 2,3-Bis(4′-(diphenylamino)-[1,1′-biphenyl]-4-yl)fumaronitrile (TPA-2CNMBE, Schemes 1c and S2 and Figure S2, SI) was newly designed and synthesized as a FRET acceptor, yielding red emission in the solid-state and characteristic AIEE properties. In addition to these fluorescent compounds, we synthesized a photochromic compound, 3,3′-(perfluorocyclopent-1-ene-1,2-diyl)bis(2-methyl-5-phenylthiophene) (open-form BP-BTE, Scheme 1d) to construct an external stimulus-responsive FRET system. BP-BTE was synthesized according to the reported procedure.[7a] Within a characteristic optical window, the absorbance of BP-BTE was negligible in either the open or closed forms.[7a,g] All new

Scheme 1. Chemical Structures of the Fluorescent Molecules: (a) CN-MBE, (b) TPS-CNMBE, and (c) TPA-2CNMBE and (d) Chemical Structure and Photochromic Reaction of BP-BTE

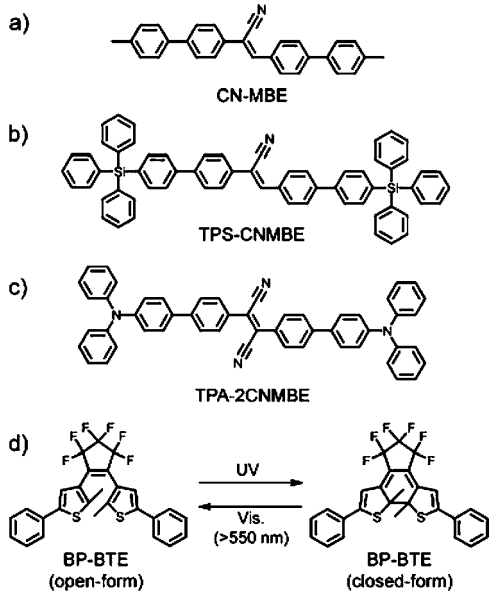

compounds were fully characterized by NMR, GC-MS, and elemental analysis (Schemes S1 and S2, SI). In this work, we endeavored to generate a highly fluorescent multicomponent chameleon nanoparticle by combining concurrent FRET and photochromic switching functions.

The FRET process between CN-MBE and TPA-2CNMBE in a two-component nanoparticle was investigated by fabricating a colloidal suspension of the compounds by the reprecipitation method,[7h,k,11e] which generates stable suspensions without surfactants by (rather kinetically controlled) spontaneous self-assembly. A mixture of the compounds in 0.5 mL tetrahydrofuran (THF) was injected rapidly into 4.5 mL water with stirring. The acceptor (TPA-2CNMBE) concentration in the mixed solution was varied from 0.1 to 50 mol % with respect to the donor (CN-MBE) concentration, while keeping the total concentration fixed at 2×10^{-5} M. The nanoparticle colloidal suspensions were exceptionally stable and did not form macroscopic precipitates, even after storing for six months.[7h,13a] DLS analysis and FE-SEM observation clearly show that average particle diameters are ranging from 255 to 296 nm at various composition (see Figure S3, SI for DLS data and Figure S4, SI for FE-SEM images). Strikingly, the nanoparticles exhibited strong fluorescence in the suspension state (quantum yield $\Phi_{F,\ donor} = 0.82$ and $\Phi_{F,\ acceptor} = 0.34$, respectively) due to their characteristic AIEE properties.

As the acceptor concentration in the nanoparticle suspension increased to 5 mol %, the donor emission was quenched dramatically, whereas the acceptor emission increased gradually with a very clear isosbestic point in the spectral evolution (Figure 2). Thus, the fluorescence color changed from greenish blue to red via white, which marked (0.21, 0.36), (0.63, 0.36), (0.36, 0.37) in the 1931 CIE coordinate diagram, respectively (Figures 2a and S5, SI). To gain insight into the FRET process, time-resolved fluorescence lifetime measurements were performed. Figure 2d shows the fluorescence decay profiles of the nanoparticle suspensions, depending on the acceptor concentration. The donor emission decay time (monitored at 472 nm)

dx.doi.org/10.1021/ja3027295 | J. Am. Chem. Soc. 2012, 134, 12091−12097

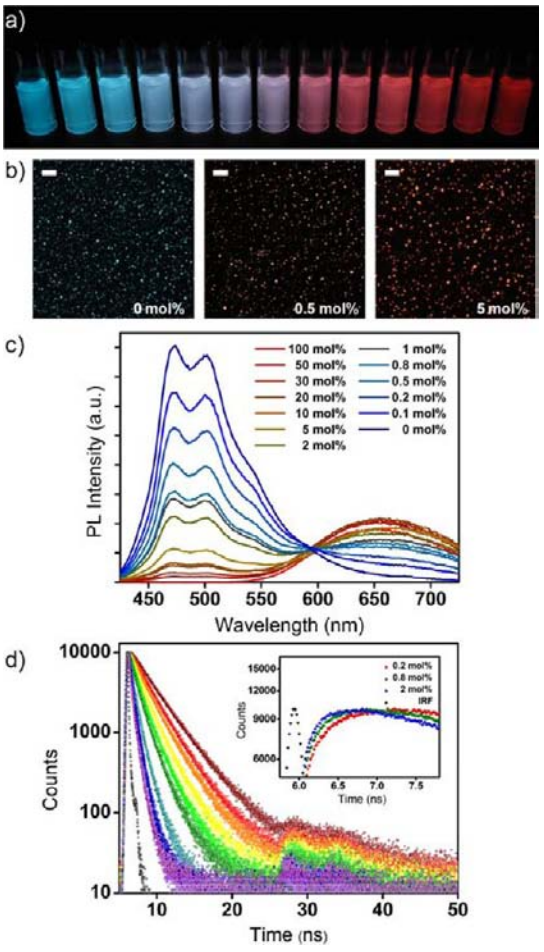

Figure 2. (a) Fluorescence images of the nanoparticle suspensions with various TPA-2CNMBE/CN-MBE molar ratios: 0, 0.1, 0.2, 0.5, 0.8, 1, 2, 5, 10, 20, 30, 50, 100 mol % TPA-2CNMBE (λ_{ex} = 365 nm). (b) Fluorescence microscopy images of nanoparticles obtained from the nanoparticle suspensions prepared with various TPA-2CNMBE/CN-MBE molar ratios: 0, 0.5, 5 mol % TPA-2CNMBE. The scale bars indicate 10 μm. (c) Fluorescence spectra of the nanoparticle suspensions with various TPA-2CNMBE/CN-MBE molar ratios: 0, 0.1, 0.2, 0.5, 0.8, 1, 2, 5, 10, 20, 30, 50, 100 mol % TPA-2CNMBE (λ_{ex} = 400 nm). (d) Fluorescence decay profiles of the nanoparticle suspensions with various TPA-2CNMBE/CN-MBE molar ratios (from wine color to purple in the full profiles): 0, 0.1, 0.2, 0.5, 0.8, 1, 2, 5, 10, 20, 30, 50 mol % TPA-2CNMBE (λ_{ex} = 377 nm; $\lambda_{monitor}$ = 472 nm in the full profiles, $\lambda_{monitor}$ = 655 nm in the inset profiles). Black points indicate the IRF values.

was markedly reduced as the acceptor ratio increased, in conjunction with the shortening of the rise time in the acceptor emission (monitored at 655 nm). Such observations clearly indicated a FRET process and the absence of trivial radiative energy-transfer processes.[14]

FRET theory predicts that efficient energy transfer is favored given good overlap between the donor emission and acceptor absorption spectra and the donor–acceptor distances smaller than the Förster radius (overlap integral $J(\lambda) = 4.50 \times 10^{14}$ M^{-1} cm^{-1} nm^4, Förster radius R_0 = 33.7 Å).[7o] The FRET efficiencies measured in our nanoparticle system were calculated to be 20%, 65%, 86%, 92% at 0.1, 1, 5, 10 mol % acceptor ratio, respectively.[2c,7o] Such high efficiencies were attributed to the excellent spectral overlap between the CN-MBE emission band (λ_{max} = 474 nm) and the TPA-2CNMBE absorption band (λ_{max} = 456 nm) (Figure S6, SI). In addition, the formation of a well-defined two-component nanoparticle via reprecipitation yielded a high FRET efficiency by facilitating intraparticle FRET.[11e] To better understand the importance of intraparticle FRET, we prepared a mixed suspension of individual donor and acceptor nanoparticles. For a given donor–acceptor ratio (1 mol % acceptor relative to the donor), the mixed nanoparticle suspensions, most likely operating through interparticle FRET and trivial energy transfer, yielded a constant greenish-blue donor emission spectrum, whereas two-component nanoparticle systems displayed white emission with an intraparticle FRET efficiency of 65% (Figure S7, SI). The properties of nanoparticles suspensions are summarized in Table 1.

Table 1. Properties of Nanoparticles Suspensions

system	Φ_F	size (nm)	FRET efficiency
CN-MBE	0.82	270	–
TPA-2CNMBE	0.34	296	–
2 comp. (1 mol %)	0.52	255	0.65
2 comp. (5 mol %)	0.33	260	0.86
2 comp. (10 mol %)	0.32	275	0.92
3 comp.[a]	0.57[b]/0.07[c]	261	0.87

[a]To simplify the system, only the close form BP-BTE was regarded as an acceptor in the three-component system. [b]Measured when BP-BTE was open form, and. [c]Close form.

The three-component nanoparticle suspension containing the photochromic molecule displayed fluorescence spectra that were tuned by photostimulus. To investigate the fluorescence color change, colloidal three-component nanoparticles were prepared via reprecipitation, as described above. A 0.5 mL THF solution of CN-MBE, TPA-2CNMBE, and the open-form BP-BTE was injected into 4.5 mL water with stirring. The molar ratios of the CN-MBE, TPA-2CNMBE, and open-form BP-BTE were fixed at 45, 5, and 50 mol %, respectively, holding the total concentration of the suspension fixed at 2×10^{-5} M. The colloidal suspension was stable and did not precipitate, even after storage for six months, similar to the two-component particle system (see Figure S3, SI for DLS data, Figure S4, SI for FE-SEM images, and Table 1 for the properties). In three-component nanoparticles, CN-MBE acted as a common donor for TPA-2CNMBE and the closed-form BP-BTE, whereas the closed-form BP-BTE acted as a nonradiative acceptor for both CN-MBE and TPA-2CNMBE. TPA-2CNMBE was used as an acceptor for CN-MBE and a donor for the closed-form BP-BTE (see Figure 3c for the energy level diagram).

Initially, a colloidal suspension of the three-component nanoparticles exhibited pink-red emission due to partial FRET from the CN-MBE to the TPA-2CNMBE. Upon UV light irradiation, the pink-red emission changed to blue via white, with 1931 CIE coordinates of (0.47, 0.33), (0.23, 0.28), and (0.32, 0.31), respectively (Figures 3a and S8, SI). The chameleon-like fluorescence color variations were attributed to color-selective quenching resulting from the photochromic transition of the open- to the closed-form BP-BTE. UV light irradiation created a broad new absorption band in the BP-BTE (λ_{max} = 590 nm), which overlapped more effectively with the emission band of TPA-2CNMBE (λ_{max} = 655 nm) than that of CN-MBE (λ_{max} = 474 nm) (Figure S6, SI). The different spectral overlap properties may have induced color tuning via fluorescence-color-selective quenching (Figure 3c). This notion was further supported by calculating the quantum chemical

dx.doi.org/10.1021/ja3027295 | J. Am. Chem. Soc. 2012, 134, 12091–12097

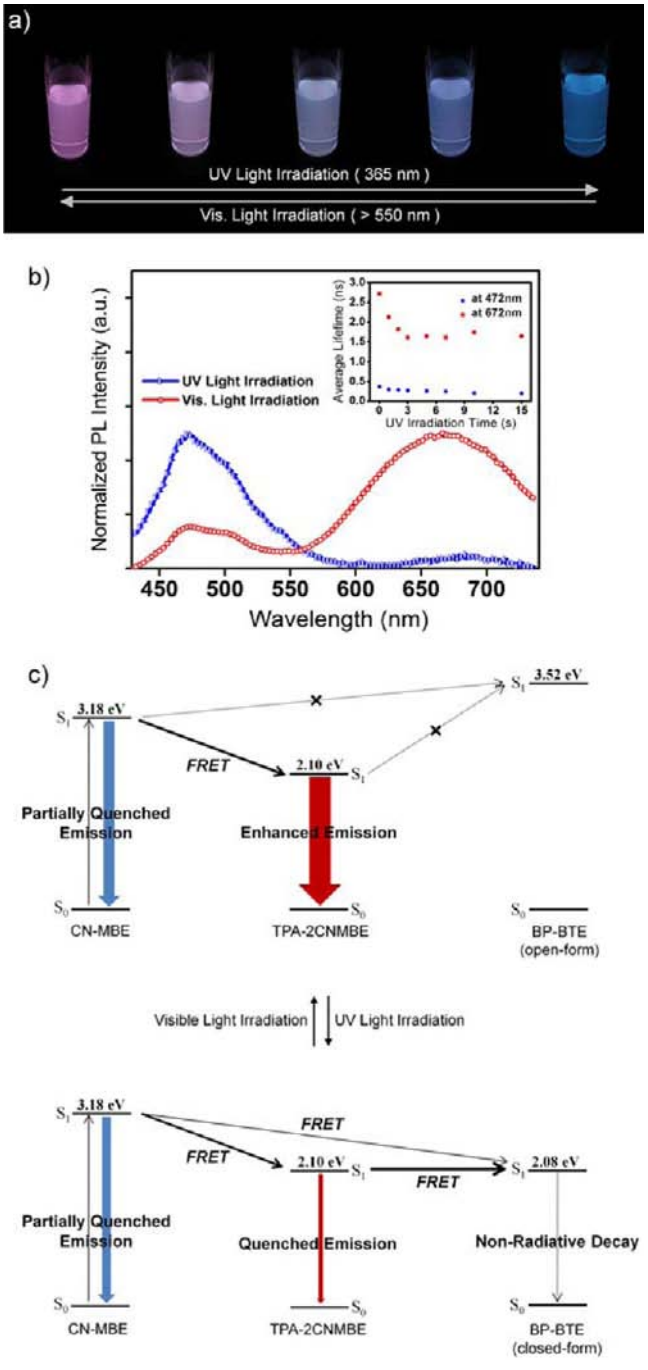

Figure 3. (a) Fluorescence images of the CN-MBE/TPA-2CNMBE/BP-BTE nanoparticle suspension upon visible or UV light irradiation (λ_{ex} = 365 nm). (b) Normalized fluorescence spectra of the CN-MBE/TPA-2CNMBE/BP-BTE nanoparticle suspension after visible and UV light irradiation (λ_{ex} = 400 nm). The inset shows the fluorescence decay profiles with increasing UV light irradiation time (λ_{ex} = 377 nm; blue points, $\lambda_{monitor}$ = 472 nm; red points, $\lambda_{monitor}$ = 672 nm). (c) Schematic illustration of the proposed FRET processes among CN-MBE, TPA-2CNMBE, and BP-BTE molecules in the CN-MBE/TPA-2CNMBE/BP-BTE nanoparticle suspension after visible and UV light irradiation.

molecular orbitals using Gaussian 9.[15] Time-dependent DFT (TD-DFT) calculations predicted excitation energy levels corresponding to the first singlet excited states of CN-MBE, TPA-2CNMBE, closed-form BP-BTE, and open-form BP-BTE of 3.18, 2.10, 2.08, and 3.52 eV, respectively. The calculation results clearly suggested that FRET from the two fluorophores to the closed-form BP-BTE should occur with different efficiencies, whereas FRET to the open-form BP-BTE was completely blocked. In fact, the closed-form of BP-BTE, generated through photocyclization, quenched 53.0% of the blue emission (λ_{max} = 474 nm) and 95.3% of the pink-red emission (λ_{max} = 672 nm) (see Figure S9, SI). The changes in the normalized emission spectra clearly showed the fluorescence color changes induced by the photostimulus (Figure 3b). The fluorescence lifetimes monitored over the emission spectral ranges of CN-MBE and TPA-2CNMBE were reduced upon UV irradiation, indicating enhanced FRET efficiencies to the closed-form BP-BTE (inset of Figure 3b).

The UV-induced fluorescence color change was completely reversed upon visible light (λ_{irr} > 550 nm) irradiation via the photochromic transition of BP-BTE to the open form. The reversibility of the fluorescent modulation was demonstrated, even upon alternating UV and visible light irradiation (Figure S9, SI). More importantly, the emission color of the three-component nanoparticles may be read without fluorescence color distortion (Figure S10, SI). The nondestructive readout properties resulted from the unique characteristics of BP-BTE, which displayed an optical window region over the range 405–440 nm, in which the absorption cross-section was negligible. Excitation at 420 nm was found to be optimal for achieving nondestructive readout, as shown in Figure S10, SI.[7g] This chameleon-like reversible fluorescence color variation property and nondestructive readout capability combined with AIEE characteristics of the fluorophores are very unique and certainly play a beneficial role in the application of this system.

For some applications, such as fluorescent optical memory, polymer films that incorporate stimulus-responsive nanostructures will be most convenient and beneficial. To explore the feasibility of such applications, we fabricated poly(methyl methacrylate) (PMMA, typical M_w = 120 000) films incorporating CN-MBE and TPA-2CNMBE and investigated their FRET characteristics. The films were fabricated by spin coating with a filtered 3 wt.% mixture containing the donor, acceptor, and polymer in 1,2-dichloroethane (DCE). The acceptor ratio was varied between 1 and 10 wt.% with respect to the donor, while the total concentration of the donor and acceptor dyes was kept at 5 wt.% with respect to the polymer. Single-component-doped polymer films were prepared for comparison to the two-component-doped polymer films. All fabricated polymer films were highly fluorescent, molecularly dispersed, uniform, and smooth without any peculiar morphological features or macroscopic aggregation (Figure S11, SI).

The fluorescence color in the film system could be fine-tuned according to the donor–acceptor composition, much like the colloidal system. As the acceptor ratio increased, the emission color changed gradually from blue to orange red through an increase in acceptor emission and a decrease in the donor emission (Figures 4a–b and S12, SI). The donor fluorescence emission lifetime and the rise time of the acceptor emission gradually decreased, clearly indicating that the emission color change corresponded to a gradual increase in the FRET efficiency (Figure S13, SI).

Interestingly, the fluorescence colors in the film system changed dramatically upon exposure to solvent vapor. To explore such changes, the polymer films were treated by SVA with dichloromethane (DCM), as shown in Figure 4a. Clearly, vapor exposure shifted the measured fluorescence spectrum of the donor–acceptor films toward the donor emission spectrum,

dx.doi.org/10.1021/ja3027295 | J. Am. Chem. Soc. 2012, 134, 12091–12097

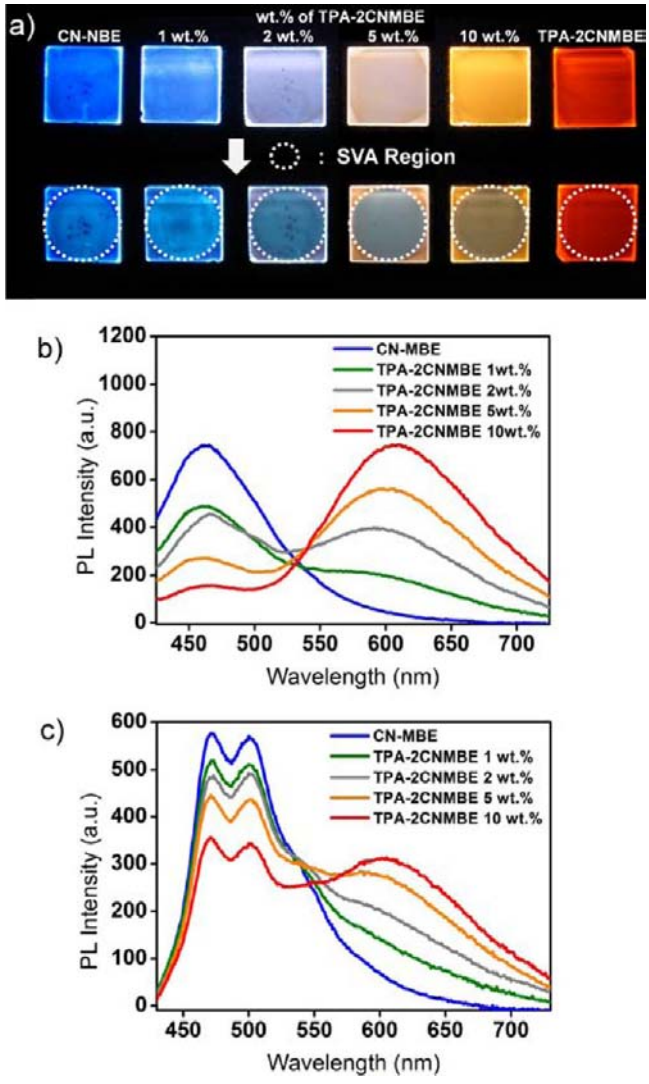

Figure 4. (a) Fluorescence images of a CN-MBE/TPA-2CNMBE-doped polymer film, showing the color modulation as a function of composition and SVA treatment (λ_{ex} = 365 nm). The concentrations of TPA-2CNMBE with respect to CN-MBE were set to 0, 1, 2, 5, 10, and 100 wt.% for films labeled CN-MBE, 1, 2, 5, and 10 wt.%, and TPA-2CNMBE, respectively. (b) Fluorescence spectra of the CN-MBE/TPA-2CNMBE-doped polymer films without any treatment, and (c) the SVA-treated CN-MBE/TPA-2CNMBE-doped polymer films with TPA-2CNMBE/CN-MBE molar ratios of 0, 1, 2, 5, 10 wt.% TPA-2CNMBE.

suggesting a significant reduction in the FRET efficiency through SVA treatment. Whereas the polymer film doped only with an acceptor (TPA-2CNMBE) was insensitive to SVA treatment (Figures 4a and S14, SI), the film doped only with a donor (CN-MBE) displayed an emission color transition from blue to greenish blue. The fluorescence spectrum of the SVA-treated polymer film resembled that of the CN-MBE nanoparticle system, indicating the generation of self-assembled aggregates from the CN-MBE/PMMA solid solution (Figures 4a–c, 2c, and S14, SI).[16] This result agreed with the optical microscopy measurements. Figure S15, SI shows that macroscopic aggregates with mean diameters of 0.1–1 μm formed over the vapor-exposed region upon SVA treatment. Similarly, SVA treatment of CN-MBE/TPA-2CNMBE-doped polymer films produced macroscopic aggregation via selective self-assembly of CN-MBE to generate bright greenish blue emission (Figures 4a–c, 2c, and S14–15, SI). Such donor-selective aggregation reduced the FRET efficiency by separating the donor from the acceptor. As a result, the donor emission increased, whereas the acceptor emission was reduced (Figures 4a–c and 2c and Table S1–2, SI) upon SVA treatment. These results agreed well with the recovered fluorescence lifetimes monitored over the donor emission wavelengths (Figure S16, SI).

To better demonstrate the self-assembly of individual donor and acceptor molecules, we prepared a CN-MBE-doped polymer film and a TPA-2CNMBE-doped polymer film using various dyes-to-PMMA doping ratios, holding the total concentration with respect to DCE constant at 3 wt.% (Figure S17–18, SI). The self-assembled particles in the CN-MBE-doped polymer film were generated by SVA treatment of films prepared with CN-MBE ratios exceeding 0.5 wt.%, whereas TPA-2CNMBE formed self-assembled aggregates upon SVA treatment of films with a TPA-2CNMBE ratio exceeding 10.0 wt.%. These observations indicate significant differences in the self-assembly properties of CN-MBE and TPA-2CNMBE, involving donor-selective aggregation. Different from the colloidal nanoparticle system, this donor-selective aggregation in the polymer film system shows the advantageous aspect for the stimulus-responsible application. However, in some applications, a response to stimuli may be seen as an instability if inertness in the presence of solvent vapor is preferred. Inertness to SVA can be realized by replacing CN-MBE with other donor fluorophores with weaker self-assembly properties. As a demonstration, we prepared a TPS-CNMBE/TPA-2CNMBE-doped polymer film. Whereas the emission color of TPS-CNMBE was the same as that of CN-MBE, the film showed a much weaker tendency to self-assemble than the CN-MBE film. The fluorescence color changed as the TPS-CNMBE/TPA-2CNMBE ratio increased, similar to the properties of the CN-MBE/TPA-2CNMBE-doped polymer film, suggesting a gradual increase in the FRET efficiency (Figure S19–23f, SI). As TPS-CNMBE/TPA-2CNMBE-doped polymer films are processed during SVA treatment, however, the film uniformity was preserved without discernible aggregation, in contrast with the CN-MBE/TPA-2CNMBE-doped polymer films. As a result, both the emission spectra and the fluorescence lifetime profiles remained unchanged. These observations clearly suggested that phase demixing through CN-MBE-selective self-assembly induced by the vapor stimulus changed the fluorescence color of the CN-MBE/TPA-2CNMBE-doped polymer films.

Finally, we demonstrated that FRET in a three-component polymer film containing donors, acceptors, and an additional photochromic molecule could be controlled by both a vapor stimulus and by photostimulus. Fluorescence color tuning was demonstrated by preparing a polymer film doped with CN-MBE, TPA-2CNMBE, and the open-form BP-BTE in a composition of 45, 5, 50 wt.%, respectively. Initially, the polymer film exhibited orange-red fluorescence attributed to partial FRET from CN-MBE to TPA-2CNMBE. Under UV light irradiation, the orange-red fluorescence color was tuned to violet-blue via white, with 1931 CIE coordinates of (0.44, 0.38), (0.27, 0.21), and (0.35, 0.30), respectively (λ_{ex} = 400 nm; Figures 5a and S24–25, SI). Obviously, fluorescence tuning was attributed to color-selective quenching due to the different FRET efficiencies from the blue or red fluorophores to the closed-form BP-BTE, as described in the context of the

dx.doi.org/10.1021/ja3027295 | J. Am. Chem. Soc. 2012, 134, 12091–12097

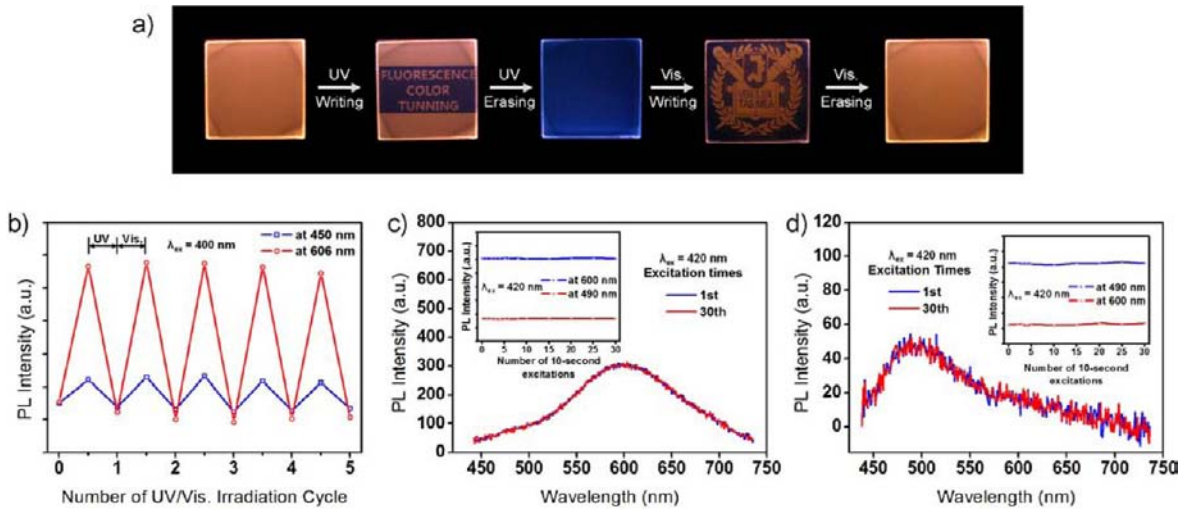

Figure 5. (a) Photoresponsive reversible fluorescence images of a CN-MBE/TPA-2CNMBE/BP-BTE-doped polymer film system (λ_{ex} = 365 nm). The orange-red and violet-blue regions represent regions irradiated with visible or UV light, respectively. (b) Reversible fluorescence color modulation of a CN-MBE/TPA-2CNMBE/BP-BTE-doped polymer film (λ_{ex} = 400 nm) under alternating UV or visible light irradiation. Fluorescence spectra (λ_{ex} = 420 nm) showing the nondestructive readout properties of CN-MBE/TPA-2CNMBE/BP-BTE-doped polymer films with (c) the open-form BP-BTE state or (d) the closed-form BP-BTE state; each inset shows the fluorescence spectra of the films at 490 and 600 nm.

nanoparticle system. BP-BTE transitions from the open-form to the closed-form under photostimulus and quenched the orange-red emission at 606 nm by 73.0%. Violet-blue emission at 450 nm was quenched by only 31.1%. The time-resolved fluorescence lifetimes were measured as a function of the UV light irradiation (Figure S26, SI). Both the donor and acceptor fluorescence lifetimes were reduced upon UV light irradiation, indicating the presence of more efficient FRET processes from both fluorescent dyes to the closed-form BP-BTE. The fluorescence color of the three-component film could be reversibly modulated using alternating UV or visible light (λ_{irr} > 550 nm, Figure 5b). In addition, the system yielded a nondestructive readout due to the optical window of BP-BTE at 420 nm, as mentioned in the context of colloidal nanoparticles. Accordingly, fluorescence emission from either the blue- or red-emitting films could be nondestructively read out using 420 nm excitation (Figure 5c,d).

The emission color of the three-component-doped polymer film could be also tuned by SVA treatment, similar to the two-component-doped polymer film system shown above. Aggregation via self-assembly of CN-MBE reduced the FRET process and shifted the emission color to a greenish blue. At this point, it is worth noting that readily distinguishable dual fluorescence pattering could be achieved by applying two different external stimuli, photo or vapor stimuli, to the film (Figure 1c). Inscription via photostimulus was reversible and ranged from violet-blue to orange-red, whereas inscription via vapor stimulus was irreversible and ranged from violet-blue to greenish-blue.

CONCLUSIONS

In summary, we prepared a system that demonstrated highly efficient stimulus-responsive fluorescence color tuning by combining the FRET with photochromic switching in self-assembled supramolecular scaffold systems. Highly fluorescent chameleon-like nanoparticles and polymer films were constructed using π-conjugated small molecules with unique AIEE characteristics as FRET donors and acceptors, together with the photochromic BP-BTE with an appropriate spectral window. Multistimulus fluorescence patterning, reversible fluorescence switching, and nondestructive readout of the fluorescence signal were successfully demonstrated in this work.

ASSOCIATED CONTENT

Supporting Information

All experimental methods and results are described; synthesis, spectroscopic data, SEM, and POM observations. This material is available free of charge via the Internet at http://pubs.acs.org.

AUTHOR INFORMATION

Corresponding Author

parksy@snu.ac.kr

Notes

The authors declare no competing financial interest.

ACKNOWLEDGMENTS

This research was supported by Basic Science Research Program (CRI; RIAMI-AM0209(0417-20090011)) and WCU (World Class University) project (R31-2008-000-10075-0) through National Research Foundation of Korea funded by the Ministry of Education, Science and Technology.

REFERENCES

(1) (a) Mitsumori, T.; Bendikov, M.; Sedó, J.; Wudl, F. *Chem. Mater.* **2003**, *15*, 3759. (b) Geng, Y.; Chen, A. C. A.; Ou, J. J.; Chen, S. H. *Chem. Mater.* **2003**, *15*, 4352. (c) Pu, Y.-J.; Higashidate, M.; Nakayama, K.; Kido, J. *J. Mater. Chem.* **2008**, *18*, 4183. (d) Kim, E.; Park, S. B. *Chem. Asian J.* **2009**, *4*, 1646. (e) Lin, S.-H.; Wu, F.-I.; Liu, R.-S. *Chem. Commun.* **2009**, 6961. (f) Abbel, R.; van der Weegen, R.; Meijer, E. W.; Schenning, A. P. H. J. *Chem. Commun.* **2009**, 1697. (g) Fukaminato, T.; Doi, T.; Tamaoki, N.; Okuno, K.; Ishibashi, Y.; Miyasaka, H.; Irie, M. *J. Am. Chem. Soc.* **2011**, *133*, 4984.

(2) (a) Adronov, A.; Gilat, S. L.; Fréchet, J. M. J.; Ohta, K.; Neuwahl, F. V. R.; Fleming, G. R. *J. Am. Chem. Soc.* **2000**, *122*, 1175. (b) Lakowicz, J. R. *Principles of Fluorescence Spectroscopy*; Springer: New York, 2006. (c) Sun, Y.; Wallrabe, H.; Seo, S.-A.; Periasamy, A. *Chemphyschem* **2011**, *12*, 462.

(3) (a) Kong, F.; Wu, X. L.; Huang, G. S.; Yuan, R. K.; Chu, P. K. *Thin Solid Films* **2008**, *516*, 6287. (b) Wu, C.; Zheng, Y.; Szymanski, C.; McNeill, J. *J. Phys. Chem. C* **2008**, *112*, 1772. (c) Bhattacharyya, S.; Paramanik, B.; Patra, A. *J. Phys. Chem. C* **2011**, *115*, 20832. (d) Jin, Y.; Ye, F.; Zeigler, M.; Wu, C.; Chiu, D. T. *ACS Nano* **2011**, *5*, 1468.
(4) (a) Wang, L.; Tan, W. *Nano Lett.* **2006**, *6*, 84. (b) Li, Z.; Zhang, Y.; Jiang, S. *Adv. Mater.* **2008**, *20*, 4765.
(5) (a) Yoo, S. I.; An, S. J.; Choi, G. H.; Kim, K. S.; Yi, G.-C.; Zin, W.-C.; Jung, J. C.; Sohn, B.-H. *Adv. Mater.* **2007**, *19*, 1594. (b) Yoo, S. I.; Lee, J.-H.; Sohn, B.-H.; Eom, I.; Joo, T.; An, S. J.; Yi, G.-C. *Adv. Funct. Mater.* **2008**, *18*, 2984.
(6) Pietsch, C.; Schubert, U. S.; Hoogenboom, R. *Chem. Commun.* **2011**, *47*, 8750.
(7) (a) Irie, M.; Lifka, T.; Kobatake, S.; Kato, N. *J. Am. Chem. Soc.* **2000**, *122*, 4871. (b) Irie, M. *Chem. Rev.* **2000**, *100*, 1685. (c) Giordano, L.; Jovin, T. M.; Irie, M.; Jares-Erijiman, E. A. *J. Am. Chem. Soc.* **2002**, *124*, 7481. (d) Irie, M.; Fukanimato, T.; Sasaki, T.; Tamai, N.; Kawai, T. *Nature* **2002**, *420*, 759. (e) Lim, S.-J.; An, B.-K.; Jung, S. D.; Chung, M.-A.; Park, S. Y. *Angew. Chem., Int. Ed.* **2004**, *43*, 6346. (f) Fukaminato, T.; Sasaki, T.; Kawai, T.; Tamai, N.; Irie, M. *J. Am. Chem. Soc.* **2004**, *126*, 14843. (g) Lim, S.-J.; Seo, J.; Park, S. Y. *J. Am. Chem. Soc.* **2006**, *128*, 14542. (h) Tian, Z.; Wu, W.; Li, A. D. Q. *ChemPhysChem* **2009**, *10*, 2577. (i) Tian, Z.; Wu, W.; Wan, W.; Li, A. D. Q. *J. Am, Chem, Soc.* **2009**, *131*, 4245. (j) Chung, J. W.; Yoon, S.-J.; Lim, S.-J.; An, B.-K.; Park, S. Y. *Angew. Chem., Int. Ed.* **2009**, *48*, 7030. (k) Tian, Z.; Yu, J.; Wu, C.; Szymanski, C.; McNeill, J. *Nanoscale* **2010**, *2*, 1999. (l) Zhu, M.-Q.; Zhang, G.-F.; Li, C.; Aldred, M. P.; Chang, E.; Drezek, R. A.; Li, A. D. Q. *J. Am. Chem. Soc.* **2011**, *133*, 365. (m) Li, A. D. Q.; Zhan, C.; Hu, D.; Wan, W.; Yao, J. *J. Am. Chem. Soc.* **2011**, *133*, 7628. (n) Deniz, E.; Tomasulo, M.; Cusido, J.; Sortino, S.; Raymo, F. M. *Langmuir* **2011**, *27*, 11773. (o) Chen, J.; Zhang, P.; Fang, G.; Yi, P.; Yu, X.; Li, X.; Zeng, F.; Wu, S. *J. Phys. Chem. B* **2011**, *115*, 3354.
(8) Wu, C.; Bull, B.; Christensen, K.; McNeill, J. *Angew. Chem., Int. Ed.* **2009**, *48*, 2741.
(9) (a) Guo, Z.; Zhu, W.; Xiong, Y.; Tian, H. *Macromolecules* **2009**, *42*, 1448. (b) Li, C.; Liu, S. *J. Mater. Chem.* **2010**, *20*, 10716. (c) Li, C.; Zhang, Y.; Hu, J.; Cheng, J.; Liu, S. *Angew. Chem., Int. Ed.* **2010**, *49*, 5120. (d) Wan, X.; Liu, S. *J. Mater. Chem.* **2011**, *21*, 10321. (e) Wang, D.; Liu, T.; Yin, J.; Liu, S. *Macromolecules* **2011**, *44*, 2282. (f) Hu, J.; Dai, L.; Liu, S. *Macromolecules* **2011**, *44*, 4699.
(10) (a) Kenworthy, A. K.; Petranova, N.; Edidin, M. *Mol. Biol. Cell* **2000**, *11*, 1645. (b) Medintz, I. L.; Clapp, A. R.; Mattoussi, H.; Goldman, E. R.; Fisher, B.; Mauro, J. M. *Nat. Mater.* **2003**, *2*, 630. (c) Sapsford, K. E.; Granek, J.; Deschamps, J. R.; Boeneman, K.; Blanco-Canosa, J. B.; Dawson, P. E.; Susumu, K.; Stewart, M. H.; Ledintz, I. G. *ACS Nano* **2011**, *5*, 2687. (d) Wang, M.; Zhang, G.; Zhang, D.; Zhu, D.; Tang, B. Z. *J. Mater. Chem.* **2010**, *20*, 1858.
(11) (a) Peng, A.-D.; Xiao, D.-B.; Ma, Y.; Yang, W.-S.; Yao, J.-N. *Adv. Mater.* **2005**, *17*, 2070. (b) Kang, L.; Chen, Y.; Xiao, D.; Peng, A.; Shen, F.; Kuang, X.; Fu, H.; Yao, J. *Chem. Commun.* **2007**, 2695. (c) Zhao, Y. S.; Fu, H.; Hu, F.; Peng, A.; Yang, W.; Yao, J. *Adv. Mater.* **2008**, *20*, 79. (d) Li, X.; Qian, Y.; Wang, S.; Li, S.; Yang, G. *J. Phys. Chem. C* **2009**, *113*, 3862. (e) Vijayakumar, C.; Sugiyasu, K.; Takeuchi, M. *Chem. Sci.* **2011**, *2*, 291.
(12) (a) Yamaguchi, S.; Yoshimura, I.; Kohira, T.; Tamaru, S.; Hamachi, I. *J. Am. Chem. Soc.* **2005**, *127*, 11835. (b) Praveen, V. K.; George, S. J.; Varghese, R.; Vijayakumar, C.; Ajayaghosh, A. *J. Am. Chem. Soc.* **2006**, *128*, 7542. (c) Zheng, J. Y.; Zhang, C.; Zhao, Y. S.; Yao, J. *Phys. Chem. Chem. Phys.* **2010**, *12*, 12935.
(13) (a) An, B.-K.; Kwon, S.-K.; Jung, S.-D.; Park, S. Y. *J. Am. Chem. Soc.* **2002**, *124*, 14410. (b) An, B.-K.; Lee, D.-S.; Lee, J.-S.; Park, Y.-S.; Song, H.-S.; Park, S. Y. *J. Am. Chem. Soc.* **2004**, *126*, 10232. (c) Yoon, S.-J.; Chung, J. W.; Gierschner, J.; Kim, K. S.; Choi, M.-G.; Kim, D.; Park, S. Y. *J. Am. Chem. Soc.* **2010**, *132*, 13675.
(14) (a) Wuister, S. F.; Koole, R.; Donegá, C.; de, M.; Meijerink, A. *J. Phys. Chem. B* **2005**, *109*, 5504. (b) Vijayakumar, C.; Praveen, V. K.; Ajayaghosh, A. *Adv. Mater.* **2009**, *21*, 2059. (c) Chen, Q.; Zhang, D.; Zhang, G.; Yang, X.; Feng, Y.; Fan, Q.; Zhu, D. *Adv. Funct. Mater.* **2010**, *20*, 3244.
(15) Frisch, M. J. et al. *Gaussian 09*, revision A.2; Gaussian, Inc.: Wallingford, CT, 2009.
(16) (a) An, B.-K.; Kwon, S.-K.; Park, S. Y. *Angew. Chem., Int. Ed.* **2007**, *46*, 1978. (b) Luca, G. D.; Liscio, A.; Nolde, F.; Scolaro, L. M.; Palermo, V.; Müllen, K.; Samori, P. *Soft Matter* **2008**, *4*, 2064. (c) Chung, J. W.; An, B.-K.; Hirato, F.; Kim, J. H.; Jinnai, H.; Park, S. Y. *J. Mater. Chem.* **2010**, *20*, 7715.